FR8902245

I.P.N. BP n°1 – 91406 ORSAY

institut de physique nucléaire CNRS - IN2P3 - UNIVERSITE PARIS - SUD

IPNO-DRE 88-23

HYPERON-NUCLEON FINAL STATE INTERACTION IN A $pp \to K^+X$ EXPERIMENT AND THE $H_1(2130)$ S = - 1 STRANGE DIBARYON

R. Frascaria[*], R. Siebert[*], J.P. Didelez[*], G. Blanpied[*], M. Boivin[**], E. Bovet[***], J.P. Egger[***], J. Ernst[+], J.Y. Grossiord[++], T. Mayer-Kuckuk[+], Ch. Perdrisat[#], B. Preedom[+++], T. Reposeur[*], B. Saghai[##], E. Warde[*], J. Yonnet[**]

[*]IPN, Orsay (France)/ [**]LNS, Saclay (France)/ [***]U. Neuchatel (Suisse)
[+]U. Bonn (RFA)/ [++]IPN Lyon (France)/ [+++]U. South Carolina (USA)
[#]Coll. William and Mary, Williamsburg (USA)/ [##]DPhN/HE, Saclay (France)

1988 International Symposium on Hypernuclear and Low-Energy Kaon Physics
Legnaro (Padova) - Italy

IPNO-DRE 88-28

HYPERON-NUCLEON FINAL STATE INTERACTION IN A $pp \to K^+X$ EXPERIMENT AND THE $H_1^+(2130)$ S = - 1 STRANGE DIBARYON

R. Frascaria[*], R. Siebert[*], J.P. Didelez[*], G. Blanpied[*], M. Boivin[**], E. Bovet[***], J.P. Egger[***], J. Ernst[+], J.Y. Grossiord[++], T. Mayer-Kuckuk[+], Ch. Perdrisat[#], B. Preedom[+++], T. Reposeur[*], B. Saghai[**], E. Warde[*], J. Yonnet[**]

[*]IPN, Orsay (France)/ [**]LNS, Saclay (France)/ [***]U. Neuchatel (Suisse)
[+]U. Bonn (RFA)/[++]IPN Lyon (France)/[+++]U. South Carolina (USA)
[#]Coll. William and Mary, Williamsburg (USA)/ [**]DPhNHE, Saclay (France)

1988 International Symposium on Hypernuclear and Low-Energy Kaon Physics
Legnaro (Padova) - Italy

HYPERON-NUCLEON FINAL STATE INTERACTION IN A $pp \to K^+X$ EXPERIMENT AND THE $H_1^+(2130)$ S = − 1 STRANGE DIBARYON

R. Frascaria[+], R. Siebert[+], J.P. Didelez[+], G. Blanpied[+], M. Boivin[++], E. Bovet[+++], J.P. Egger[+++], J. Ernst[†], J.Y. Grossiord[††], T. Mayer-Kuckuk[†], Ch. Perdrisat[#], B. Preedom[†††], T. Reposeur[+], B. Saghai[**], E. Warde[+], J. Yonnet[++]

[+] *IPN, Orsay (France)/* [++]*LNS, Saclay (France)/* [+++]*U. Neuchatel (Suisse)*
[†]*U. Bonn (RFA)/* [††]*IPN Lyon (France)/* [†††]*U. South Carolina (USA)*
[#]*Coll. William and Mary, Williamsburg (USA)/* [**]*DPHNHE, Saclay (France)*

I - SHORT REPORT ON THE H_1^+

It has been known for a long time from the study of the reaction $K^-d \to \pi^- \Lambda p$ that a structure exists in the Λp missing mass spectra near the Σ^+n threshold (M_{Σ^+n} = 2129 MeV). Some spectra from the main K^-d experiments are shown in Fig. 1. All these experiments yield a structure for which position and width are very similar. They are presented in Table 1 with the main experimental conditions. This was the experimental situation around 1980. Such a signal, called H_1^+ (2130), needed new studies to clarify its nature as a "*kinematical*" or "*dynamical*" effect. Two new experiments then came out both bringing confirmations of such a structure.

The first one (Ref. 7) performed at CERN produced the strange dibaryonic H_1^+ system in the reaction $K^-d \to \pi^-H_1^+$, and the line-reversed reaction $\pi^+d \to K^+ H_1^+$ between 0.9 and 1.4 GeV/C. The two reactions were done at three different beam setting 1.4, 1.06 and 0.92 GeV/c for the (K^-d) experiment and 1.4, 1.2 and 1.06 GeV/c for the (π^+ d) experiment. The analysis of these data, on which we will come back later lead to a H_1^+, the characteristics of which are :

$$(1)\ M = 2129.8 \pm 0.2 \pm 2\ \text{MeV}/c^2 \text{ and}$$
$$\Gamma = 16.7 \pm 1.9 \pm 2\ \text{MeV}/c^2.$$

A typical spectrum for the $\pi^+ d \to K^+ X$ reaction is shown in Fig. 2. The dotted curve corresponds to the H_1^+ Breit Wigner resonance.

The second new experiment was the AGS experiment 773 at BNL (Ref. 8). This experiment studied the reaction $K^-d \rightarrow \pi^- X$ at 870 MeV/c incident momentum for pion angles ranging from 9 to 27°. A large bump was observed corresponding to the sum of two peaks, one located at 2129 MeV, the other centered at 2139 MeV. We will not discuss here this second peak appearing as a shoulder in the main peak centered at 2129 MeV ; one can only note that these two peaks were already present in the bubble chamber experiment performed by Tan et al. (Ref. 1). This second peak at 2138.8 ± 0.7 MeV with Γ = 9.1 ± 2.4 MeV has been presented in Ref. 8 as a good candidate for the $Q^4 \otimes Q^2$ six quark triplet state named D_T predicted by Aerts et al.(Ref.9). The differential cross section for the peak centered at 2129 MeV follows the expected slope for a S state production.

To sum up the present experimental situation a clear signal for a two baryon state (S = - 1) is observed in the Λp-invariant mass of these K^-d or $\pi^+ d$ reactions at 2.129 ± 0.03 GeV. The origine of this structure is unfortunately less clear : this is due to the fact that the opening of the Σ^+n at 2.129 and $\Sigma^0 p$ at 2.131 GeV channels produce cusps at these invariant masses. Thus a detailed analysis of the reaction has to be done to *disentangle the kinematical cusp effects from dynamical effects.* Many studies have been done on this subject and a complete review up to 1980 can be found in a report by Dalitz (Ref. 10).

Dosh and Stamatescu (Ref. 25) have calculated the conversion process $\Sigma N \rightarrow \Lambda N$ in the $K^-d \rightarrow \Lambda p \pi^-$ reaction (Fig. 3, graph b) with also a nucleon exchange term (Fig. 3 graph a). The $YN \rightarrow \Lambda p$ amplitudes are obtained by a K-matrix formalism with a further constraint given by the measured cross sections of the processes $\Sigma^- p \rightarrow \Lambda n$, $\Sigma^- p \rightarrow \Sigma^0 n$, $\Sigma^- p \rightarrow \Sigma^- p$ and $\Sigma^+ p \rightarrow \Sigma^+ p$. The results of this calculation are shown in Fig. 4a in comparison with the experimental results of Ref. 3 and Ref. 6. In Fig. 4b, the calculation has been performed with constant hyperon-nucleon scattering amplitudes, showing that the agreement can only be achieved by introducing a structure into the hyperon-nucleon scattering amplitudes.

Hemming and Morris (Ref. 16) in an OBE model have calculated the $K^-d \rightarrow \Lambda p \pi$ cross sections for K^- in flight and at rest including the mass differences within the Σ and N multiplets. There are six different channels in the YN interaction for coupled $^3S_1$ and $^3D_1$. These amplitudes are calculated with both BDI-1 and BDI-2 potentials of Ref. 13. The best agreement with the data of Ref. 1 and Ref. 3 is obtained with the BDI-1 potential which has a ΛN resonance just below the ΣN threshold. As shown in Fig. 5, Dalitz and Deloff (Ref. 17) have yielded the same agreement with the *NRS-F* potential of Ref. 11, which also predicts a Λp resonance.

Pigot et al. (Ref. 7) analysing their own CERN results on both $K^-d \to \pi^- X$ and $\pi^+ d \to K^+X$ reactions following the procedure of Dosh et al. reach the same conclusion : if the triplet YN scattering amplitude in the conversion $\Sigma N \to \Lambda N$ process is taken constant the calculation is not sufficient to fully account for the experimental data. It is particularly true for the $\pi^- d \to K^+ X$ reaction at 1.4-1.2 GeV/c. They introduce a H_1^+ dibaryon represented by a Breit-Wigner shape and obtained the mass and width mentioned above. With a resonance centered at 2130 MeV, they are able to reproduce the energy dependence of the production rate at 180° c.m.s. for both reactions at the same time.

Kerbikov et al. (Ref. 13) have performed a P-matrix analysis of the low energy YN interactions within the *Jaffe-Low formalism* (Ref. 14). Analysing the enhancement of the Λp invariant mass near the $\Sigma^+ n$ threshold they conclude that it should be identified as a P-matrix partner of the deuteron. The pole lies at $M_{pole} = (2.127 - i\ 0.00168)$ GeV and may be called a ΣN bound state and a Λp resonance. Bakker et al. (Ref. 15) found in a two-channel approximation a similar result.

Presently the result of all these investigations is that the amplitude of the reaction $K^-d \to \Lambda N \pi$ does have a pole close to the $\Sigma^+ n$ threshold, the origin of which is in the YN interactions and then appearing in all the amplitudes of the reactions $YN \to YN$. The analysis of the data, mainly those of Ref. 1 and Ref. 3, favors the YS 3DI-1 and NRS-F potentials which both have a ΛN resonance just below the $\Sigma^+ n$ threshold.

II - THE $pp \to K^+X$ EXPERIMENT

As discussed before, the use of different reactions or kinematical conditions can help to clarify the nature of the H_1^+. In this sense, the $pp \to K^+ X$ reaction is a simple system in which the hyperon-nucleon interaction can be studied through final state interaction (FSI) between the two baryons in the output channel, and thus any effect in the YN system can be observed.

A $pp \to K^+X$ experiment was performed at BNL in 1968 (Ref. 23) which was statistically accurate but suffered from a poor K^+ momentum resolution and bad *absolute momentum determination. This experiment* showed a strong FSI just above the Λp (2054 MeV) threshold in the Λp missing mass spectra taken at $\theta_K = 0$ for two different incident proton energies ($T_p = 2.35$ and 2.4 GeV). In these poor experimental conditions no enhancement was observed in the dibaryon missing mass around the $(\Sigma N)^+$ threshold.

A new pp → K^+X experiment has been performed at the Saturn National laboratory (LNS) with high resolution to study Λp and ΣN FSI in a large range of momentum transfer and missing mass. The experiment utilizes the SPES4 beam line. The experimental set up has been given elsewhere (Ref. 19). The SPES4 beam line is a 32 meter long spectrometer which allows the momentum analysis of particle up to 4 GeV/c ; the solid angle of the spectrometer is $\Delta\Omega = 2.5.10^{-4}$ with momentum acceptance $\Delta p/p = \pm 3.5$ % and momentum resolution 10^{-4}. The protons and pions are partly rejected by means of total reflection Cerenkov detectors. The discrimination between particles (protons, pions and kaons) is obtained by velocity measurements over a 16 meter flight path.

Using multidrift chambers, reconstruction of particle trajectories are done at the focal plane and a missing mass spectrum is obtained. The results of this investigation include cross sections for K^+ emission at $\theta_K = 0°$, 6, 8, 10 and 12°, K^+ for protons of 2.3 GeV. The θ_K = 6, 8, 10 and 12° missing mass spectra are shown in Fig. 6. The error bars are only statistical. The spatial resolution in the dispersive plane is of the order of 0.5 mm, leading to a momentum resolution for the retracing of about 0.25 MeV/c. at 1200 MeV/c. The energy losses in the target and in the scintillators at the intermediate focal plane and the multiple scattering yields an energy straggling of 1.5 MeV (FWHM). This has been checked on $^{12}C(p,p')$ low level excitations. The presented missing mass spectra, shown, are the result of a convolution of the data by 2.5 MeV bins.

The three spectra for θ_K = 8°, 10°, 12° showing the same shape and absolute cross sections have been added and are shown in Fig. 7 . The dashed curve represents the 3-body phase spaces (3-BPS) of the reactions (1), (2) and (3). The error bars are only statistical. The energy bin width is 1.5 MeV corresponding to the experimental resolution. One observes two different regions as compared to the 3-BPS :

- the Λp mass region where the 3-BPS is strongly distorted by the Λ-p FSI. The full line in figure 7 shows preliminary calculations of the pp → K^+ Λp differential cross section at zero degree within the one kaon exchange mechanism based upon an older work on pion production off nuclei (Ref. 26). The Λp FSI was parametrized in the s-wave by a separable potential with parameters adjusted to a scattering length a and an effective range r_0 identical for the singlet and triplet s-state ($a = -1.8$ fm, $r_0 = 3.42$ fm).

- the $(\Sigma N)^+$ mass region where a structure peaked around 2130 MeV appears at the threshold. This structure is shown at the bottom of figure 7 as a result of the subtraction of the 3 BPS from the data. It is the first time that such a structure is observed in a $pp \to K^+X$ reaction.

Its position and width can be deduced from a Breit Wigner shape fit. The result is : $M = 2131 \pm 1.5$ MeV and $\Gamma = 9 \pm 1$ MeV. The integrated cross section for its production in this $pp \to K^+X$ experiment at $E_p = 2.3$ GeV and for $\theta_K = 10 \pm 2°$ is of the order of 500 nb/sr. This production rate is comparable to the one found in th $\pi^+ d \to K^+ H_1^+$ reaction and one order of magnitude smaller than in the $K^- d \to \pi^- H_1^+$ reaction studied in the experiment of Ref. 7. This production rate is closely related to the momentum transfer which is low in the (K,π) experiment but rather high in the (π,K) and (p,K^+) experiments.

In order to separate the different contributions that could participate in the formation of this structure a calculation of the mechanism of the reaction has to be performed. In the basic meson production process traditionally a meson exchange model is employed and fair agreement with experiments has been achieved in the case of pion production where extensive data can be found. In the case of kaon production early calculations done in the 1960's (Ref. 27) showed that the kaon exchange mechanism dominates the $pp \to K^+ \Lambda p$. The skeleton of this mechanism is shown in Fig. 8 graph a. The dominance of the K^+ exchange term over the π^+ exchange term (Fig. 8, graph b) can be simply understood if a comparison between the products $G_{p\to K^+\Lambda} \times \sigma(K^+p \to K^+p)$ and $G_{p\to\pi^+N} \times \sigma(\pi^+p \to \Lambda K^+)$ is done. The two coupling constants $G_{NN\pi}/\sqrt{4\pi} = 3.3$ and $G_{NK\Lambda}/\sqrt{4\pi} = 4$ are near the same but $\sigma(K^+p \to K^+p)$ ($\cong$ 10 mb) dominates over $\sigma(\pi^+p \to \Lambda K^+)$ ($\leqslant$ 1 mb) by a factor of ten in the kaon momentum range $0.1 < pK < 1$ GeV/c. The YN final state interaction (FSI) leads to triangle diagrams c) and d) of Fig. 8 respectively in K^+ and π^+ meson exchange, where Y is either the Σ or Λ hyperon. An interesting point is that in graph c, the coupling constant $N \to YK$ is needed, its value beeing -4.07 for $N\Lambda K$ and 0.26 for $N\Sigma K$ (Ref. 11) : in the case of K meson exchange a Λ is mainly produced and the FSI is predominantly a $\Lambda p \to \Lambda p$ process. This dynamical situation is very different in the case of the $K^- d \to \Lambda p K^+$ reaction where the triangle OPE diagram (Fig. 2) is dominated by $\Sigma N \to \Lambda N$ conversion term. Moreover, the lower part of the $H_1^+(2130)$ is not perturbated by the Fermi momentum distribution of the nucleons in the deuterium as in the $d(K,\pi)$ or $d(\pi,K)$ experiments. The $\Lambda p \to \Lambda p$ cross section has been calculated by Nagels et al. (Ref. 11) in a general baryon-baryon description in terms of one-boson-exchange potentials where SU(3) relations are assumed for the coupling of the different mesons. The result of this calculation for the Λp elastic cross sections is shown in Fig. 9 for two different potentials

NRS-D and NRS-F. The NRS-F is constraint by more physical inputs and is theoretically improved compared to the NRS-D one. The NRS-F potential leads to a pole in the $^3S_1$ amplitude which can be related to the deuteron pole in the $^3S_1$ NN amplitude. The real part of the pole position is 0.98 MeV above the Σ^+p threshold energy. As one can see in the figure, the elastic experimental data are very scarce in the vicinity of the $(\Sigma N)^+$ thresholds and cannot help to make a choice between the two potentials. A complete calculation of graphs a) and c) of Fig. 8 are in progress (Ref. 24).

To conclude, as mentioned by Dalitz (Ref. 10) the difficulty to explain this cusp effect is related to the large SU(3) breaking. This is clearly shown for instance in the baryon-baryon potential studies performed by Nagels et al. (Ref. 11) where following a OBE model, the physical meson and baryon masses are used in local potentials due to exchange of members of the pseudoscalar, vector and scalar-meson monets. This analysis leads to the prediction of a pole in the $^3S_1$ YN amplitude near the ΣN threshold : the strong cusp observed in the $S = -1$ channel should correspond to the $S = 0$ deuteron. This does not allow to conclude that there is a ΛN resonance. The more recent and more complete potentiel (NRS-F) from Nagels et al. predicts such a resonance. Its existence of course strongly depends on the pole position. The only way to go further is to get more ΛN scattering data. The $\Lambda p \rightarrow \Lambda p$ data are very scarce in the vicinity of the ΣN threshold. The $pp \rightarrow K^+X$ experiment provides a good mean to get these informations. This kind of reaction involves large momentum transfer but yields production rate of the same order than in the $d(\pi,K)$ reaction. The different kinematical conditions in the incoming channel (K meson exchange dominance, no deuteron Fermi momentum) should suppress the $\Sigma N \rightarrow \Lambda N$ conversion process and help to disentangle the kinematical from the dynamical effects. A detailed analysis of the process is needed and is in progress. From a pure experimental point of view, more exclusive $pp \rightarrow K^+X$ experiments such as $pp \rightarrow K^+\Lambda p$ and $pp \rightarrow K^+\Sigma^+n$ reactions have to be studied. Transfer polarisation to the hyperon can also be studied in polarized proton scattering. All these experiments can be done at LNS where a strangeness production program is scheduled.

REFERENCES

1) TAI HO TAN, Phys. Rev. Lett. 23(1969)395
2) D. CLINE et al., Phys. Rev. Lett. 20(1968)1452
3) O. BRAUN et al., Nucl. Phys. B124(1977)45
4) W.H. SIMS et al., Phys. Rev. D3(1971)1152
5) G. ALEXANDER et al., Phys. Rev. Lett. 22(1969)483
6) D. EASTWOOD et al., Phys. Rev. D3(1971)2603
7) C. PIGOT et al., Nucl. Phys. B249(1985)172
8) M. PIEKARZ et al., Int. Symp. on hypernuclei and kaon PMMS BNL, sept. 85
9) A.T.M. AERTS, P.J.G. MULDERS and J.J. DESWART, Phys. Rev. D17(1978)260 ; D19(1979)2635 ; D21(1980)1370 and 2653
10) R.H. DALITZ, Nucl. Phys. A354(1981)101C
11) M.M. NAGELS et al., Phys. Rev. D12(1975)744 ; D15(1977)2547, D20(1979)1633
12) R.H. DALITZ and S.F. TUAN, Ann. Phys. (N.Y.) 10(1960)307
13) B.O. KERBIKOV et al., Nucl. Phys. A480(1988)585
14) R.L. JAFFE and F.E. LOW, Phys. Rev. D19(1979)2105
15) B.L.G. BAKKER et al., Sov. J. Nucl. Phys. 43(1986)982
16) R.H. DALITZ, C.R. HEMMING, E.J. MORRIS, Nukleonika, 25(1980)1555
17) R.H. DALITZ and A. DELOFF, CZECH, J. Phys. B32(1982)1021
18) J.T. BROWN et al., Nucl. Phys. B47(1972)138
19) R. FRASCARIA, R. SIEBERT, Few-Body Systems, Supp. 2 (1987)425 ; R. SIEBERT, R. FRASCARIA et al., Nucl. Phys A479(1988)389C.
20) O.I. DAHL, Phys. Rev. Lett. 6(1961)142
21) D.P. GOYAL et al., Phys. Rev. D18(1978)948
22) D.P. GOYAL et al., Prog. of Theor. Physics 64(1980)700
23) M. MAY et al., Phys. Rev. C25(1982)1079
24) J.M. LAGET, Private communication.
25) H.G. DOSH and I.O. STAMATESCU, Z. Phys. C3(1980)249
26) J.F. GERMOND and C. WILKIN, J. Phys. G11(1985)1131 ; see also Ref. 19
27) E. FERRARI, Phys. ReV. 120(1960)988
28) J.T. REED et al., Phys. Rev. 168(1968)1495

Figure caption

Fig. 1 : Missing mass spectra obtained in different $K^-d \rightarrow \Lambda p \pi^-$ experiments (Ref. 1-6)

Fig. 2 : Missing mass spectrum of the reaction $\pi^+ d \rightarrow K^+ X$ at 1.4 GeV/c. The dotted curve is for the H_1^+ contribution. M_T is the multiplicity cut (from Ref. 7)

Fig. 3 : Skeleton diagrams for the reaction $K^-d \rightarrow \pi^- \Lambda p$ taken into account in the calculation of Ref. 25

Fig. 4 : Calculated missing mass spectra in the reaction $K^-d \rightarrow \pi^- \Lambda p$ in comparison with the data of Ref. 3 and 6 (respectively up and down figures)
Fig. 4a : Set (I) of K-matrix elements
Fig. 4b : constant hyperon-nucleon amplitudes (from Ref. 25)

Fig. 5 : Result of the calculation of Dalitz and Deloff with two different hyperon nucleon potentials (NRS-F : Ref. 11, BDI-1 : Ref. 18) in comparison of the at rest $K^-d \rightarrow \Lambda p \pi^-$ data of Ref. 1 (from Ref. 17)

Fig. 6 : The LNS missing mass spectra of the reaction $pp \rightarrow K^+ X$ at E_p = 2.3 GeV, for θ_K = 6, 8, 10 and 12°.

Fig. 7 : The summed missing mass spectrum between 3 and 12° from Fig. 6. The data in the lower part of the figure are the result of the subtraction of the 3 BPS to the experimental data in the (ΣN) missing mass region. The full line in the Λp mass region is the calculation of the Λp FSI in the impulse approximation from Ref. 26

Fig. 8 : Diagrams for the $pp \rightarrow K^+ X$ reaction in
Fig. 8a and b : respectively K-meson and π-meson exchange without baryon baryon rescattering
Fig. 8c and d : Respectively K-meson and π-meson exchange with Y-N FSI

TABLE I

Experimental observations of the H_1^+(2130) till 1980.

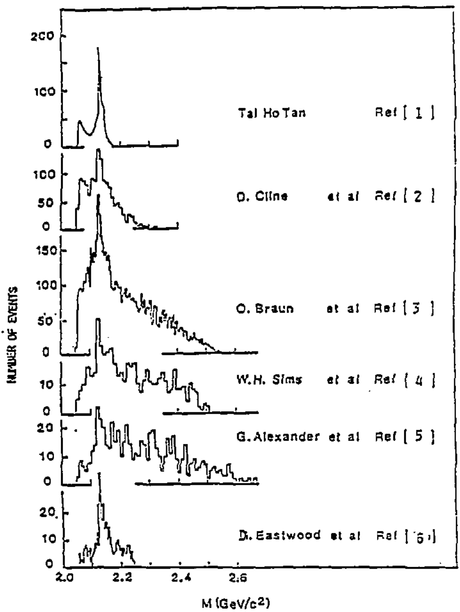

200
100
0
50
150
10
20
NUMBER OF EVENTS
Tai Ho Tan Ref [1]
D. Cline et al Ref [2]
O. Braun et al Ref [3]
W.H. Sims et al Ref [4]
G. Alexander et al Ref [5]
D. Eastwood et al Ref [6]
2.0
2.2
2.4
2.6
M (GeV/c2)

Fig. 1

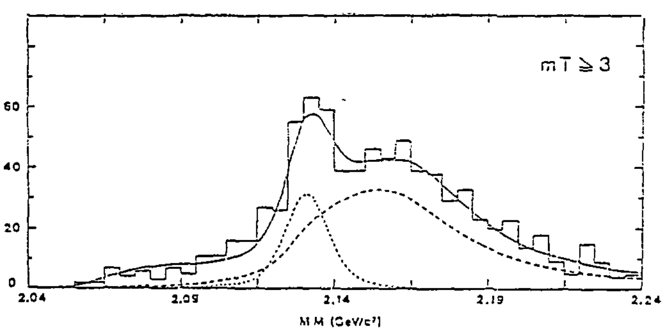

mT ≥ 3
60
40
20
0
2.04
2.09
2.14
2.19
2.24
MM (GeV/c²)

Fig. 2

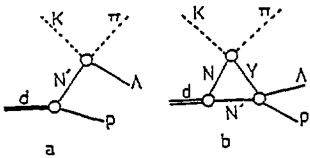

Fig. 3

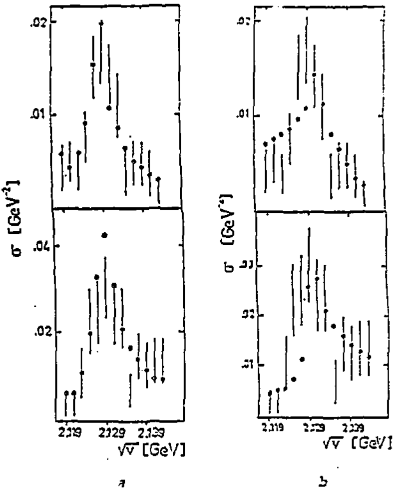

Fig. 4

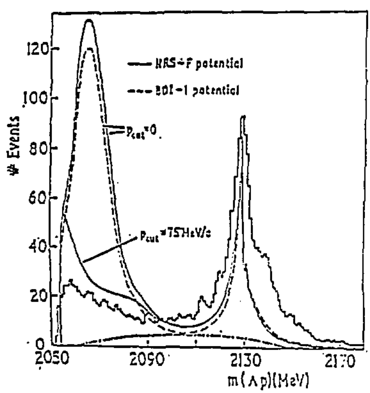

Fig. 5

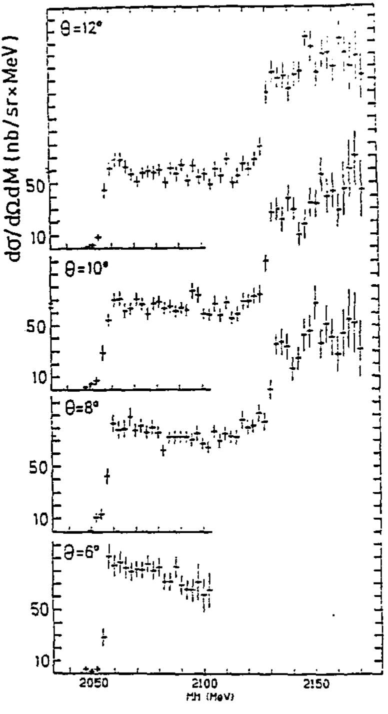

dσ/dΩdM (nb/sr×MeV)
θ=12°
θ=10°
θ=8°
θ=6°
50
10
50
10
50
10
50
10
2050
2100
2150
MM (MeV)

Fig. 6

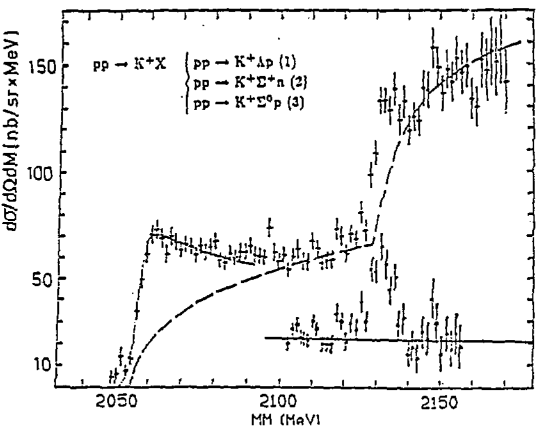

pp → K⁺X
pp → K⁺Λp (1)
pp → K⁺Σ⁺n (2)
pp → K⁺Σ⁰p (3)
dσ/dΩdM(nb/sr×MeV)
150
100
50
10
2050
2100
2150
MM (MeV)

Fig. 7

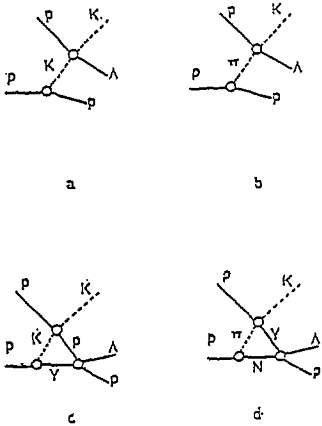

Fig. 8

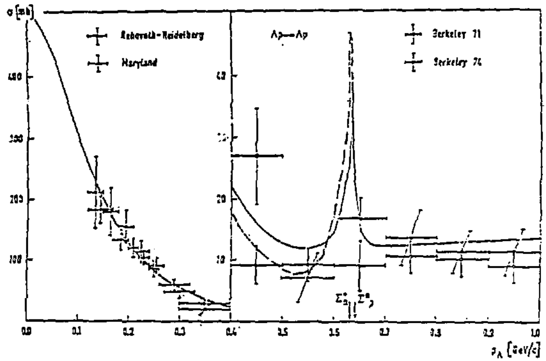

Fig. 9

References	Reaction	Incident momentum GeV/c	Resolution MeV/c²	Number of events	Observation in the missing mass (YN) MeV/c²	Width MeV/c²
O.I. Dahl et al. Ref. 20	Bubble chamber $K^-d \rightarrow \pi^-(\Lambda p)$	$\leq$ .45	-	300	2130	-
D. Cline et al. Ref. 2	Bubble chamber $K^-d \rightarrow \pi^-(\Lambda p)$	.4	-	1400	2126.	< 10.
G. Alexander et al. Ref. 5	Bubble chamber $K^-d \rightarrow \pi^-(\Lambda p)$	.91 1.007 et 1.106	3.	560 (with momentum cut on spectator)	2130.	-
Tai Ho Tan Ref. 1	Bubble chamber $K^-d \rightarrow \pi^-(\Lambda p)$	Stopped kaons	1.	2470	2128.7 ± .2 ; 2138 ± .7	7. ± 6 / 9.1 ± 2.4
			2.6	2431	idem	idem
W.H. Sims et al. Ref. 4	Bubble chamber $K^-d \rightarrow \pi^-(\Lambda p)$ $\pi\pi(\Lambda N)$	from .67 to .925	-	2600	2127. ± 1. en (Λp) et (Λn)	3. ± 1.
D. Eastwood et al. Ref. 6	Bubble chamber $K^-d \rightarrow \pi^-(\Lambda p)$	1.45 and 1.65	3.	4000 (with momentum cut on spectator)	2129.	10.
O. Braun et al. Ref. 3	Bubble chamber $K^-d \rightarrow \pi^-(\Lambda p)$	.68 $\leq p \leq$ .84	2.	9600	2129. ± 4. a shoulder till 2180.	5.9 ± 1.6
D.P. Goyal et al. Ref. 21	Bubble chamber $K^-d \rightarrow \pi^+\pi^-\pi^-(\Lambda p)$	1.45 et 1.65	-	2500.	2130. et un effet à 2200.	-
D.P. Goyal et al. Ref. 22	Bubble chamber $K^-d \rightarrow \pi^0\pi^+\pi^-(\Sigma^-p)$	1.45 and 1.65	-	1500 and 2400	2301. ± 5.	21. ± 16.
M. May et al. Ref. 23	$K^-d \rightarrow \pi^- + X^+$ $(\theta^*_{K\pi} = 4°)$	.8	4.	3300	Event exces at ΣN threshold	-

TABLE I